



Bidirectional DC to DC converter for Hybrid Electric vehicles using Fuzzy logic controller

M.Murali | V. Gangadhar | J.V.V. Krishna Chaitanya | Ch. Siva Ganesh

Department of Electrical & Electronics Engineering, Godavari Institute of Engineering and Technology (A), JNTUK, Kakinada

To Cite this Article

M.Murali | V. Gangadhar, J.V.V. Krishna Chaitanya and Ch. Siva Ganesh. Bidirectional DC to DC converter for Hybrid Electric vehicles using Fuzzy logic controller. International Journal for Modern Trends in Science and Technology 2022, 8(S02), pp. 30-38. <https://doi.org/10.46501/IJMTST08S0206>

Article Info

Received: 26 April 2022; Accepted: 24 May 2022; Published: 30 May 2022.

ABSTRACT

This paper organizes a application of hybrid electric vehicle systems operated with novel designed bidirectional dc-dc converter (BDC) which interfaces a main energy storage (ES1), an auxiliary energy storage (ES2) and dc bus of different voltage levels. Proposed BDC converter can operate both step up and step down mode. In which step up mode represents low voltage dual source -powering mode and step down mode represents high voltage dc link energy –regenerating mode, both the modes are operated under the control of bidirectional power flow. This model can independently control power flow between low voltage dual source buck/boost modes. Here in, the circuit configuration, operation, steady-state analysis, and closed-loop control of the proposed BDC are discussed according to its three modes of power transfer. In this project fuzzy logic controller is used and also system results are validates through MATLAB/SIMULINK software.

Index Terms—Bidirectional dc/dc converter (BDC), dual battery storage, hybrid electric vehicle, Fuzzy logic controller.

1.INTRODUCTION

Overall natural change and energy supply is declining have animated changes in vehicular development. For the applications in later vehicles the cutting edge innovations are at present being researched. Among such applications, power module mixture electric vehicles (FCV/HEV) are productive and promising competitors. Previously, Ehsani et al. concentrated on the vehicles' elements to search for an ideal force speed profile of the electric impetus framework [1]. Emadi et al. discussed the functioning properties of the topographies for different vehicles including HEV, FCV, and more electric vehicles [2]. To fulfill enormous vehicular burden, for cutting edge vehicular power framework Emadi et al. additionally incorporated power gadgets serious arrangements [3]. Schaltz et al. adequately partition the heap power among the power module stack, the battery,

and the ultra capacitors in light of two proposed energy-the executives methodologies [4]. Thounthong et al. studied the effect of power module (FC) execution and the advantages of hybridization for control frameworks [5]. Chan et al. audited electric, mixture, and power module vehicles and focused on designs and displaying for energy the board [6]. Khaligh and Li presented energy-capacity geographies for HEVs and module HEVs (PHEVs). They additionally examined and analyzed battery, UC, and FC advancements. Additionally, they likewise tended to different half breed ESSs that incorporate at least two stockpiling gadgets [7]. Rajashekara discussed the stream status and the necessities of fundamental electric drive parts-the battery, the electric engines, and the power hardware framework [8]. Lai et al. executed a bidirectional dc/dc converter

geography with two-stage and interleaved characteristics.

The Voltage Transformation proportion of the converter has worked on in the EV and DC miniature framework frameworks. Furthermore, Lai additionally analyzed a bidirectional dc to dc converter (BDC) geography which has a high voltage change proportion for EV batteries related with a dc-miniature framework [10]. In FCV frameworks, the essential battery stockpiling gadget is usually used to start the FC and to supply capacity to the drive engine [2, 3].

The battery stockpiling gadgets further develop the intrinsically sluggish reaction time for the FC stack through providing top power during speeding up the vehicle [7]. Also, it contains a powerful thickness part for instance, super capacitors (SCs) dispense with top power drifters during speeding up and regenerative slowing down [11]. As a rule, SCs can store regenerative energy during deceleration and delivery it during speed increase, subsequently providing extra power. The powerful thickness of SCs drags out the life expectancy of both FC stack and battery stockpiling gadgets and works on the general effectiveness of FCV systems.

This examination proposes an interleaved voltage-doublers structure [9, 28] and a coordinated buck-help circuit are a two new BDC geographies for FCV/HEV power framework. It features two fundamental working modes: a low-voltage twofold source-driving mode and a high-voltage dc-transport energy-recovering mode. Moreover when the converter is in low-voltage double source buck-help mode the proposed converter can freely control power stream between any two low-voltage sources. A comparable geography was introduced in [29] that simply talk about a short thought. Then again, this examination presents itemized investigation of the activity and shut circle control of this new geography as well as reenactment results for every one of its methods of activity. The proposed converter can work over a more extensive scope of voltage levels that is the reason this study extended the geography introduced in [29].

The principle attributes of the proposed converter are summed up as follows:

- Interfaces multiple dc hotspots for different voltage levels,

- Controls power stream between the dc transport and the two low-voltage sources and besides freely controls power stream between the two low-voltage sources,
- Enhances static voltage gain and therefore decreases switch voltage stress, and
- Possesses a sensible duty cycle and makes a wide voltage distinction between its high-and low-side ports.

A practical chart for a regular (FCV/HEV) power framework is represented in Fig. 1 [4, 13]. The low-voltage FC stack is utilized as the fundamental power source, and SCs straightforwardly associated in corresponding with FCs. The dc/dc power converter is utilized to change over the FC stack voltage into an adequate dc-transport voltage in the driving inverter for providing capacity to the impetus engine. Moreover, ES1 with rather higher voltage is utilized as the fundamental battery stockpiling gadget for providing top power, and ES2 with rather lower voltage could be a helper battery capacity gadget to accomplish the vehicle range extender idea [13]. The capacity of the bidirectional dc/dc converter (BDC) is to communicate double battery energy capacity with the dc-transport of the driving inverter. By and large, the FC stack and battery stockpiling gadgets have different voltage levels. A few multiport BDCs have been created to give explicit voltages to burdens and control power stream between various sources, hence decreasing generally speaking expense, mass, and power utilization [14-27]. These BDCs can be ordered into detached and non separated types.

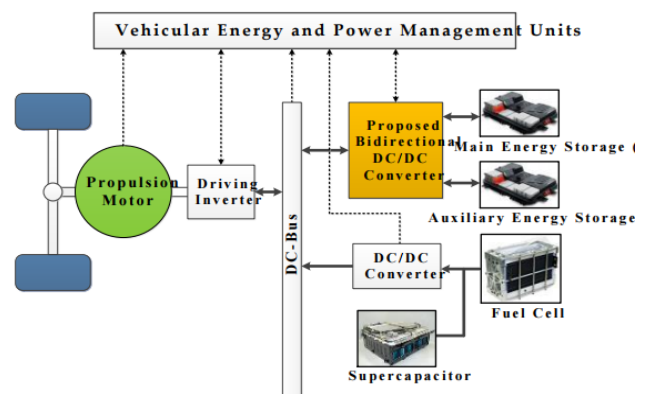


Fig.1. Typical functional diagram for a FCV/HEV power system.

In detached converters, high-recurrence power transformers are applied to empower galvanic confinement. A couple secluded multiport BDC geographies have been explored, for example, the fly

back, half-or full-span circuits, double dynamic scaffolds, and resounding circuits . The writing recommends that non disengaged BDCs are more compelling than common separated BDCs in EVs .Liu et al. determined non detached multi-input converter geographies via a blend of buck, support, Ćuk, and Sepic. In [23], Wu et al. fostered the three-port non disconnected multi-input-multi-yeild (MIMO) converter geographies for interacting a sustainable source, a capacity battery, and a heap all the while. The three twofold info converters created in [19] include a solitary post triple-toss switch and just a single inductor. A secluded non disconnected MIMO converter was introduced . This converter is applied to hybridize clean energy wellsprings of EVs and the fundamental lift circuit was altered furthermore, incorporated. Nonetheless, the voltage gain of the MIMO help circuit is restricted by and by, due to the misfortunes related for certain parts, for example, the primary influence switch, inductor, channel capacitor, and rectifier diode.

To overcome this drawback, three-port power converter that has high-gain characteristic and contains FC, battery sources and stacked output for interfacing HEV, as well as a dc-micro grid was presented. Although the multiport BDC discussed,can interface more than two sources of power and operate at different voltage levels, it still has limited static voltage gains, resulting in a narrow voltage range and a low voltage difference between the high and low-side ports.

2. PROPOSED TOPOLOGY

The proposed BDC geography with double battery energy capacity is outlined in Fig.1, where V_H , V_{ES1} , and V_{ES2} address the high-voltage dc-transport voltage, the primary energy stockpiling (ES1), and the helper energy capacity (ES2) of the framework, individually. Two bidirectional power switches (SES1 and SES2) in the converter structure, are utilized to turn on or switch off the ongoing circles of ES1 and ES2, separately. A charge-siphon capacitor (CB) is coordinated as a voltage divider with four dynamic switches (Q_1, Q_2, Q_3, Q_4) and two stage inductors (L_1, L_2) to further develop the static voltage gain between the two low-voltage double sources (V_{ES1}, V_{ES2}) and the high-voltage dc transport (V_H) in the proposed converter. Moreover, the extra CB decreases the switch voltage stress of dynamic switches and dispenses with the need to work at an outrageous

obligation proportion. Moreover, the three bidirectional power switches ($S, SES1, SES2$) showed in Fig. 2 display four-quadrant activity and are taken on to control the power stream between two low-voltage double sources (V_{ES1}, V_{ES2}) and to impede either certain or negative voltage.

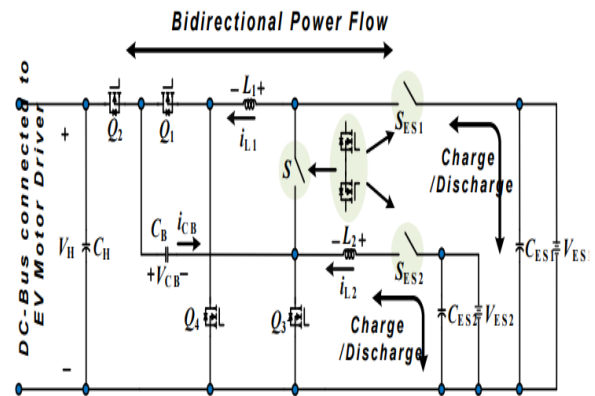


Fig.2.1. Proposed BDC topology with dual-battery energy storage.

This bidirectional power switch is carried out through two metal-oxide-semiconductor field-impact semiconductors (MOSFETs), pointing in inverse bearings, in series association. To make sense of the idea for the proposed converter, all the conduction situations with the power gadgets engaged with every activity mode are shown in Table 2.1. In like manner, the four working modes are delineated as follows to upgrade understanding..

TABLE 2.1. CONDUCTION STATUS OF DEVICES FOR DIFFERENT OPERATING MODES

Operating Modes	ON	OFF	Control Switch	Synchronous Rectifier (SR)
Low-voltage dual-source-powering mode (Accelerating, $x_1=1, x_2=1$)	S_{ES1}, S_{ES2}	S	Q_2, Q_4	Q_1, Q_3
High-voltage dc-bus energy-regenerating mode (Braking, $x_1=1, x_2=1$)	S_{ES1}, S_{ES2}	S	Q_1, Q_3	Q_2, Q_4
Low-voltage dual-source buck mode (ES1 to ES2, $x_1=0, x_2=0$)	S_{ES1}, S_{ES2}	Q_1, Q_2, Q_4	S	Q_3
Low-voltage dual-source boost mode (ES2 to ES1, $x_1=0, x_2=0$)	S_{ES1}, S_{ES2}	Q_1, Q_2, Q_4	Q_3	S
System shutdown	-	S_{ES1}, S_{ES2} Q_1, Q_2, Q_3, Q_4	-	-

2.1. Low-Voltage Dual-Source-Powering Mode

Fig. 2.2(a) portrays the circuit schematic and consistent state wave structures for the converter under the low-voltage double source-fueling mode. In that, the switch S is switched off, and the switches ($SES1, SES2$) are turned on, and the two low-voltage double sources (V_{ES1}, V_{ES2}) are providing the energy to the dc-transport and loads. In this mode, the low-side switches Q_3 and Q_4 are effectively exchanging at a stage

shift point of 180°, and the high-side switches Q1 and Q2 work as the coordinated rectifier (SR). In view of the common wave forms displayed in Fig. 2.2(b), when the obligation proportion is bigger than half, four circuit states are conceivable (Fig. 2.2). In the illumination of the on/off status of the dynamic switches and the working guideline of the BDC in low-voltage double source-driving mode, the activity can be made sense of momentarily as follows.

State 1 [t0 < t < t1]: During this express, the time span (1-Du) Tsw, switches Q1, Q3 are turned on, and switches Q2, Q4 are switched off. The voltage across L1 is the contrast between the low-side voltage VES1 and the charge-siphon voltage (VCB), and consequently iL1 diminishes straightly from the underlying worth. Likewise, inductor L2 is charged by the energy source VES2,

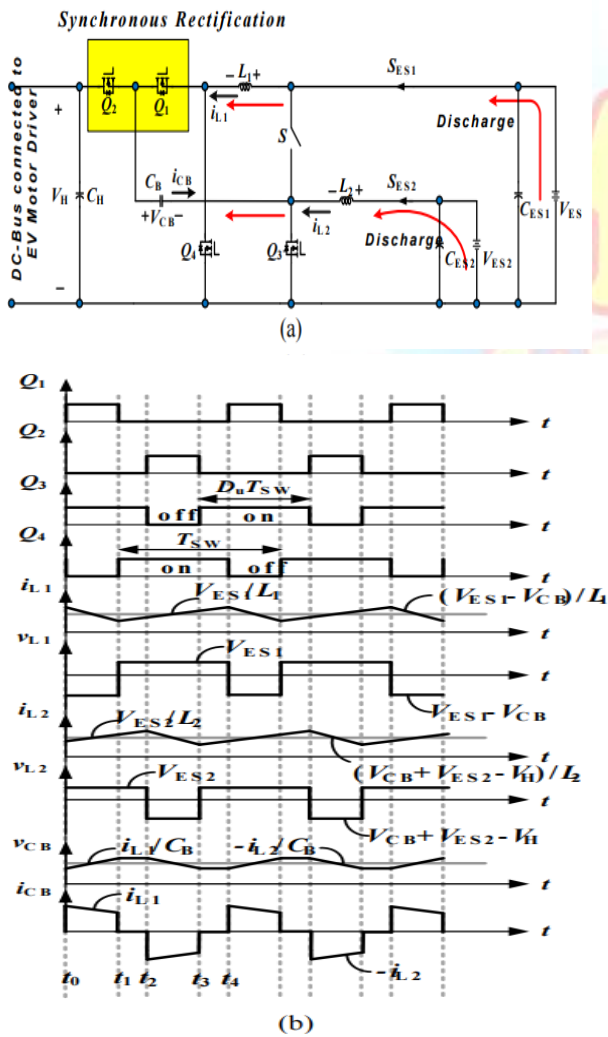


Fig. 2.2. Low-voltage dual-source-powering mode of the proposed BDC: (a) circuit schematic and (b) steady-state waveforms.

consequently producing a direct expansion in the inductor current. The voltages across inductors L1 and L2 can be meant as

$$L_1 \frac{di_{L1}}{dt} = V_{ES2} - V_{CB} \quad (1)$$

$$L_2 \frac{di_{L2}}{dt} = V_{ES2} \quad (2)$$

State 2 [t1 < t < t2]: During this express, the interval time is (Du-0.5)Tsw; switches Q3 and Q4 are turned on; and switches Q1 and Q2 are turned.

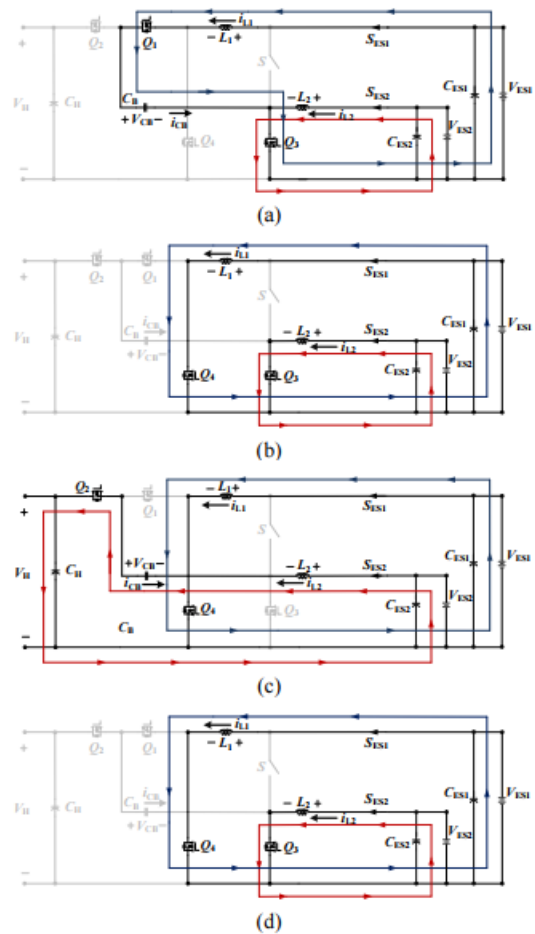


Fig. 2.3 Circuit states of the proposed BDC for the low-voltage dual-source-powering mode. (a) State 1. (b) State 2. (c) State 3. (d) State 4.

a) off. The low-side voltages VES1 and VES2 are situated between inductors L1 and L2, separately, consequently straightly expanding the inductor flows, and starting energy to capacity. The voltages across inductors L1 and

L2 under state 2 can be meant as

$$L_1 \frac{di_{L1}}{dt} = V_{ES1} \quad (3)$$

$$L_2 \frac{di_{L2}}{dt} = V_{ES2} \quad (4)$$

b) State 3 [$t_2 < t < t_3$]: During this state, the interval time is $(1-D_u)T_{sw}$; switches Q1 and Q3 are turned on, whereas switches Q2 and Q4 are turned off. The voltages across inductors L1 and L2 can be denoted as

$$L_1 \frac{di_{L1}}{dt} = V_{ES1} \quad (5)$$

$$L_2 \frac{di_{L2}}{dt} = V_{CB} + V_{ES2} - V_H \quad (6)$$

c) State 4 [$t_3 < t < t_4$]: During this state, the interval time is $(D_u - 0.5)T_{sw}$; switches Q3 and Q4 are turned on, and switches Q1 and Q2 are turned off. The voltages across inductors L1 and L2 can be denoted as

$$L_1 \frac{di_{L1}}{dt} = V_{ES1} \quad (7)$$

$$L_2 \frac{di_{L2}}{dt} = V_{ES2} \quad (8)$$

2.2. High-Voltage DC-Bus Energy-Regenerating Mode :

In this mode, the dynamic energy put away in the engine drive is taken care of back to the source during regenerative slowing down activity. The regenerative power can be a lot higher than whatever the battery can retain. Thus, the overabundance energy is utilized to charge the energy stockpiling gadget. The circuit schematic and the consistent state waveforms of the BDC under the high-voltage dc transport energy-recovering mode are shown in Fig.2.4.

In that, the current in the inductors is constrained by the dynamic switches Q1 and Q2, which have a stage shift point of 180° and along these lines direct the stream away from the dc-transport and toward the double energy stockpiling gadgets; the switches Q3 and Q4 work as the SR to further develop the change effectiveness.

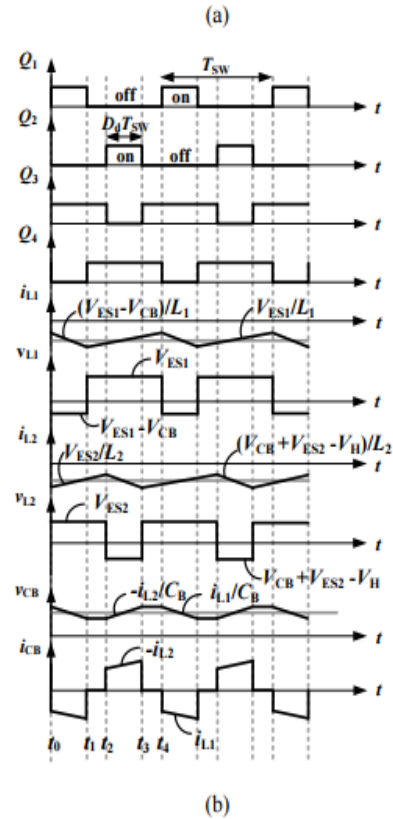
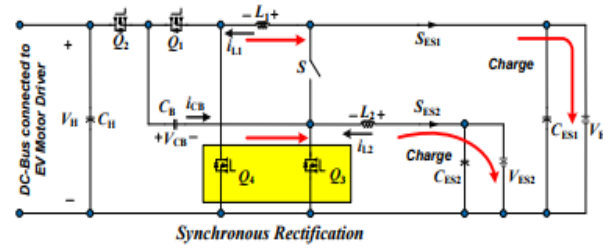


Fig.2.4. High-voltage dc-bus energy-regenerating mode of the proposed BDC: (a) circuit schematic and (b) steady-state waveforms.

Based on the consistent state waveforms displayed in Fig. 2.4(b), when the obligation proportion is underneath half, four different circuit states are conceivable, as displayed in Fig. 2.5. In the radiance of the on-off status of the dynamic switches and the working guideline of the BDC in high-voltage dc-transport energy-recovering mode,

the activity can be portrayed momentarily as follows.

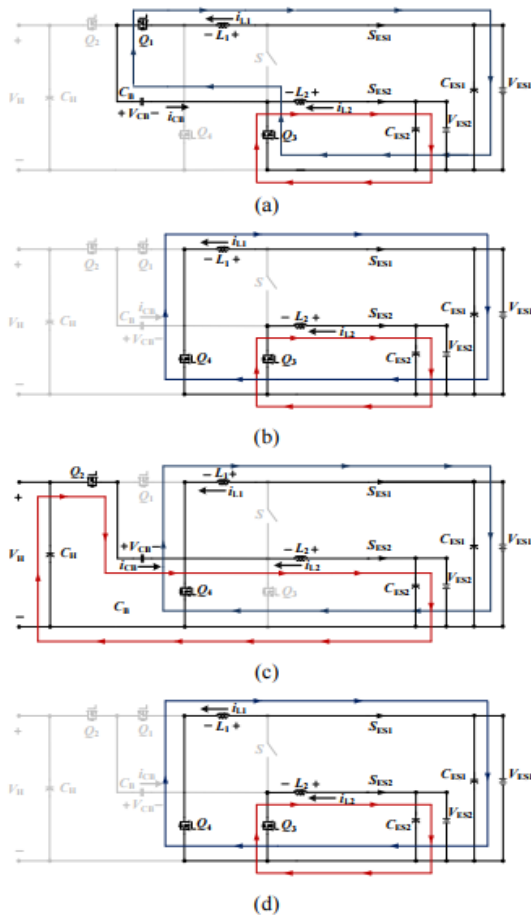


Fig. 2.5. Circuit states of the proposed BDC for the high-voltage dc-bus energy-regenerating mode. (a) State 1. (b) State 2. (c) State 3. (d) State 4.

a) State 1 [$t_0 < t < t_1$]: During this express, the timespan $Dd Tsw$; switches Q1 and Q3 are turned on, and switches Q2 and Q4 are switched off. The voltage across L1 is the contrast between the low-side voltage V_{ES1} and the charge-siphon voltage V_{CB} ; thus, the inductor current i_{L1} diminishes directly from the underlying worth. Likewise, inductor L2 is charged by the energy source.

b) V_{ES2} , which additionally adds to the direct expansion in the inductor current. The voltages across inductors L1 and L2 can be indicated as

$$L_1 \frac{di_{L1}}{dt} = V_{ES1} - V_{CB} \quad (9)$$

$$L_2 \frac{di_{L2}}{dt} = V_{ES2} \quad (10)$$

c) State 2 [$t_1 < t < t_2$]: During this state, the interval time is $(0.5-Dd)Tsw$; switches Q3 and Q4 are turned on, and switches Q1 and Q2 are state off. The voltages across inductors L1 and L2 are the positive the low-side voltages V_{ES1} and V_{ES2} , respectively; hence, inductor currents

i_{L1} and i_{L2} increase linearly. These voltages can be denoted as

$$L_1 \frac{di_{L1}}{dt} = V_{ES1} \quad (11)$$

$$L_2 \frac{di_{L2}}{dt} = V_{ES2} \quad (12)$$

c) State 3 [$t_2 < t < t_3$]: During this express, the time frame $Dd Tsw$; switches Q1 and Q3 are switched off, and switches Q2 and Q4 are turned on. The voltage across L1 is the positive low-side voltage V_{ES1} and consequently i_{L1} increments directly from the underlying worth. Also, the voltage across L2 is the distinction of the great side voltage V_H , the charge-siphon voltage V_{CB} , and the low-side voltage V_{ES2} , and its level is negative. The voltages across inductors L1 and L2 can be meant as

$$L_1 \frac{di_{L1}}{dt} = V_{ES1} \quad (13)$$

$$L_2 \frac{di_{L2}}{dt} = V_{ES2} + V_{CB} - V_H \quad (14)$$

d) State 4 [$t_3 < t < t_4$]: During this express, the time frame is $(0.5-Dd)Tsw$; switches Q3 and Q4 are state on, and switches Q1 and Q2 are state off. The voltages across inductor L1 and L2 can be denoted as

$$L_1 \frac{di_{L1}}{dt} = V_{ES1} \quad (15)$$

$$L_2 \frac{di_{L2}}{dt} = V_{ES2} \quad (16)$$

Remaining modes of operation were explained in [1].

3. FUZZY CONTROLLER:

The word Fuzzy means unclearness. Fluffiness happens when the limit of snippet of data isn't obvious. In 1965 Lotfi A. Zahed propounded the fluffy set hypothesis. Fuzzy set hypothesis displays monstrous potential for compelling tackling of the vulnerability in the issue. Fuzzy set hypothesis is an incredible numerical instrument to deal with the vulnerability emerging because of ambiguity. Grasping human discourse and perceiving transcribed characters are a few normal examples where fluffiness shows.

Fuzzy set hypothesis is an expansion of traditional set hypothesis where components have differing levels of enrollment. Fuzzy rationale utilizes the entire span somewhere in the range of 0 and 1 to depict human thinking. In FLC the info factors are planned by sets of participation capacities and these are called as "Fuzzy SETS".

Fuzzy set involves from a participation work which could be characterizes by boundaries. The worth somewhere in the range of 0 and 1 uncovers a level of enrollment to the fuzzy set. The most common way of switching the fresh contribution over completely to a fluffy worth is called as "fuzzificaton." The result of the Fuzzier module is communicated with the standards. The fundamental activity of FLC is built from fuzzy control rules using the upsides of fuzzy sets overall for the mistake and the difference in blunder and control activity. Fundamental fluffy module is displayed in fig.5 The outcomes are consolidated to give a fresh result controlling the result variable and this interaction is called as "DEFUZZIFICATION."

4.1 MATLAB CIRCUITS:

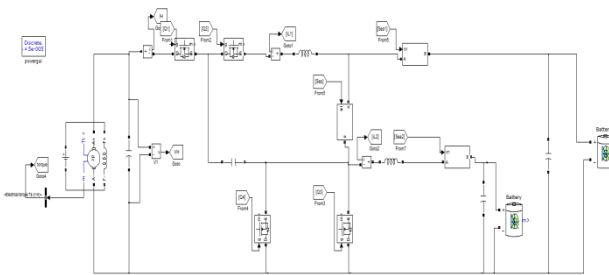


Fig4.1 Simulation Block Diagram

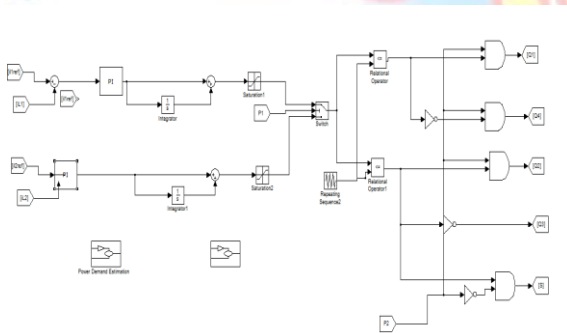


Fig4.2 Simulation Control Diagram

4.2 WAVE FORMS:

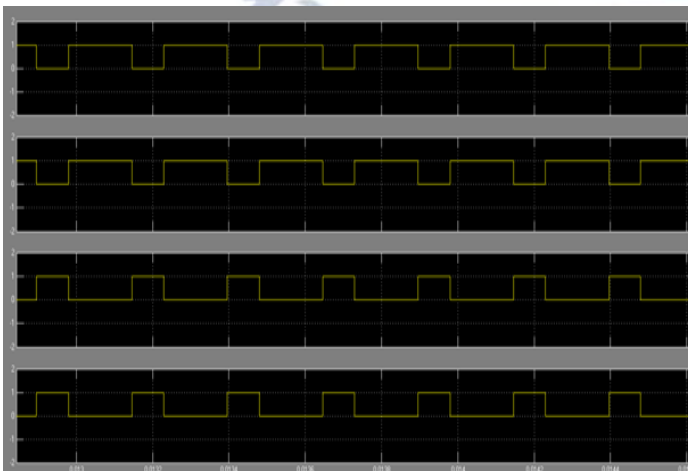
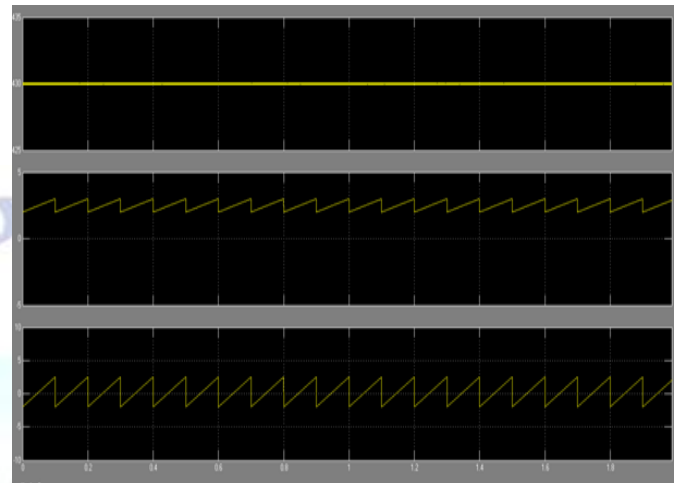


Fig. 4.3. Measured waveforms for low-voltage dual-source-powering mode:(a) gate signals



(b) output voltage and inductor currents.

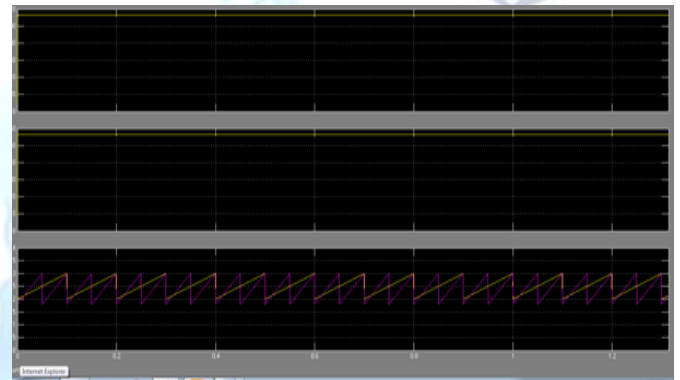


Fig. 4.4. Measured waveforms for high-voltage dc-bus energy-regenerating mode:.

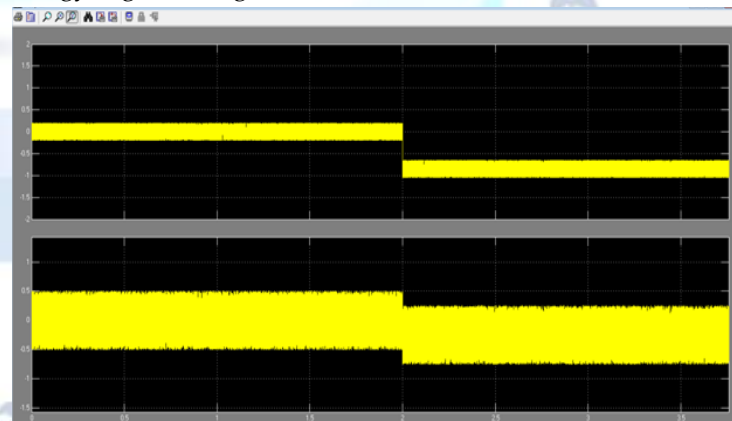


Fig.4.5. Waveforms of controlled current step change in the low-voltage dual-source-powering mode by simulation

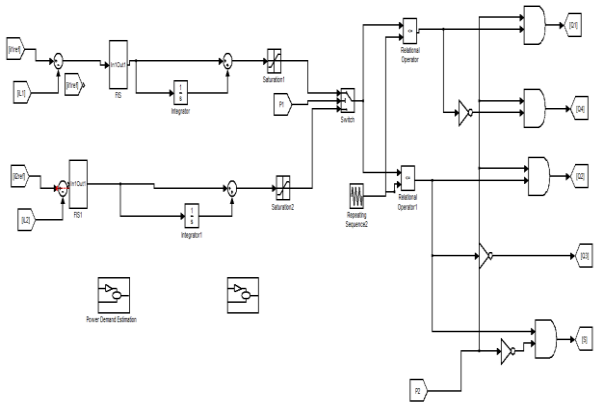


Fig4.6 Simulation of fuzzy logic Control Diagram

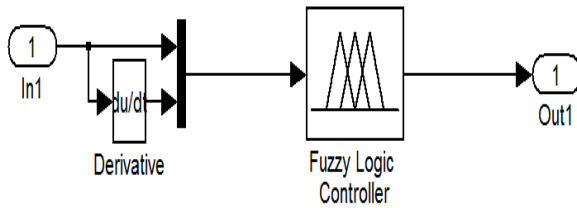


Fig4.7 fuzzy logic Controller

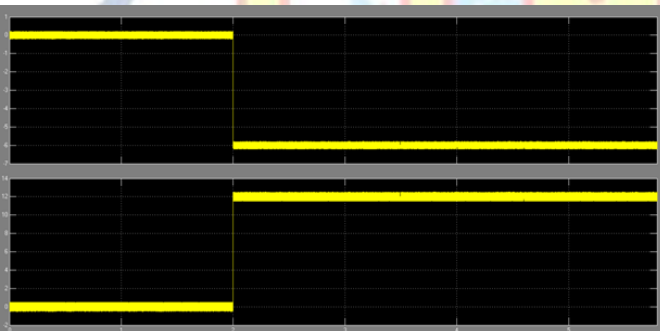


Fig. 4.8 Waveforms of controlled current step change in the low-voltage dual-source boost mode: by simulation;

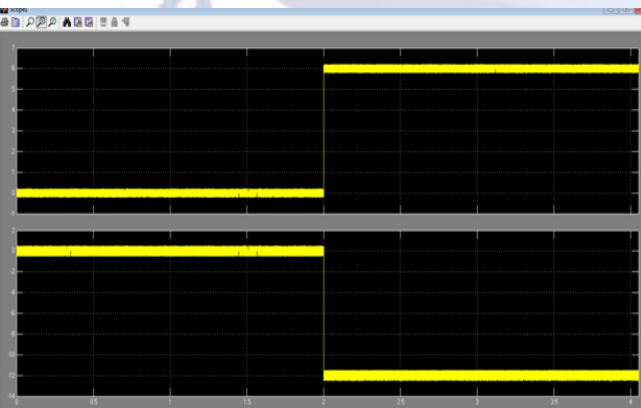


Fig. 4.9 Waveforms of controlled current step change in the low-voltage dual-source buck mode: by simulation

5. CONCLUSION

A Another BDC geography was introduced to connect double battery energy sources and high-voltage dc transport of various voltage levels. The circuit setup, activity standards, examinations, and static voltage gains of the proposed BDC were talked about based on various methods of force move. Reproduction waveforms for a 1 kW model framework featured the presentation and practicality of this proposed BDC geography. The most noteworthy change efficiencies were 97.25%, 95.32%, 95.76%, and 92.67% for the high-voltage dc-transport energy-regenerative buck mode, low-voltage double source-controlling mode, low-voltage double source help mode (ES2 to ES1), and low-voltage double source buck mode (ES1 to ES2), separately. In this paper fluffy rationale regulator is utilized to upgrade the proposed geography. The outcomes exhibit that the proposed BDC can be effectively applied in FC/HEV frameworks to create half and half power engineering.

Conflict of interest statement

Authors declare that they do not have any conflict of interest.

REFERENCES

- [1] Ching-Ming Lai, Member, IEEE, Yu-Huei Cheng, Senior Member, IEEE, Ming-Hua Hsieh, and Yuan-Chih Lin" Development of a Bidirectional DC/DC Converter with Dual-Battery Energy Storage for Hybrid Electric Vehicle System" 2017 IEEE
- [2] M. Ehsani, K. M. Rahman, and H. A. Toliyat, "Propulsion system design of electric and hybrid vehicles," IEEE Transactions on industrial electronics, vol. 44, no. 1, pp. 19-27, 1997.
- [3] A. Emadi, K. Rajashekar, S. S. Williamson, and S. M. Lukic, "Topological overview of hybrid electric and fuel cell vehicular power system architectures and configurations," IEEE Transactions on Vehicular Technology, vol. 54, no. 3, pp. 763-770, 2005.
- [4] A. Emadi, S. S. Williamson, and A. Khaligh, "Power electronics intensive solutions for advanced electric, hybrid electric, and fuel cell vehicular power systems," IEEE Transactions on Power Electronics, vol. 21, no. 3, pp. 567-577, 2006.
- [5] P. Thounthong, V. Chunkag, P. Sethakul, B. Davat, and M. Hinaje, "Comparative study of fuel-cell vehicle hybridization with battery or supercapacitor storage device," IEEE transactions on vehicular technology, vol. 58, no. 8, pp. 3892-3904, 2009.
- [6] C. C. Chan, A. Bouscayrol, and K. Chen, "Electric, hybrid, and fuel-cell vehicles: Architectures and modeling," IEEE transactions on vehicular technology, vol. 59, no. 2, pp. 589-598, 2010.
- [7] A. Khaligh and Z. Li, "Battery, ultracapacitor, fuel cell, and hybrid energy storage systems for electric, hybrid electric, fuel cell, and plug-in hybrid electric vehicles: State of the art," IEEE transactions on Vehicular Technology, vol. 59, no. 6, pp. 2806-2814, 2010.
- [8] K. Rajashekar, "Present status and future trends in electric vehicle propulsion technologies," IEEE Journal of Emerging and Selected Topics in Power Electronics, vol. 1, no. 1, pp. 3-10, 2013.
- [9] C.-M. Lai, Y.-C. Lin, and D. Lee, "Study and implementation of a two-phase interleaved bidirectional DC/DC converter for vehicle

- and dc-microgrid systems," *Energies*, vol. 8, no. 9, pp. 9969-9991, 2015.
- [10] C.-M. Lai, "Development of a novel bidirectional DC/DC converter topology with high voltage conversion ratio for electric vehicles and DC-microgrids," *Energies*, vol. 9, no. 6, p. 410, 2016.
- [11] J. Moreno, M. E. Ortúzar, and J. W. Dixon, "Energy-management system for a hybrid electric vehicle, using ultracapacitors and neural networks," *IEEE transactions on Industrial Electronics*, vol. 53, no. 2, pp. 614-623, 2006.
- [12] J. Bauman and M. Kazerani, "A comparative study of fuel-cell-battery, fuel-cell-ultracapacitor, and fuel-cell-battery-ultracapacitor vehicles," *IEEE Transactions on Vehicular Technology*, vol. 57, no. 2, pp. 760-769, 2008.
- [13] M. Ehsani, Y. Gao, and A. Emadi, *Modern electric, hybrid electric, and fuel cell vehicles: fundamentals, theory, and design*. CRC press, 2009.
- [14] Z. Haihua and A. M. Khambadkone, "Hybrid modulation for dual active bridge bi-directional converter with extended power range for ultracapacitor application," in *Industry Applications Society Annual Meeting, 2008. IAS'08. IEEE, 2008*, pp. 1-8: IEEE.
- [15] H. Tao, J. L. Duarte, and M. A. Hendrix, "Three-port triple-half-bridge bidirectional converter with zero-voltage switching," *IEEE transactions on power electronics*, vol. 23, no. 2, pp. 782-792, 2008.
- [16] T. Bhattacharya, V. S. Giri, K. Mathew, and L. Umanand, "Multiphase bidirectional flyback converter topology for hybrid electric vehicles," *IEEE Transactions on Industrial Electronics*, vol. 56, no. 1, pp. 78-84, 2009.
- [17] H. Krishnaswami and N. Mohan, "Three-port series-resonant DC-DC converter to interface renewable energy sources with bidirectional load and energy storage ports," *IEEE Transactions on Power Electronics*, vol. 24, no. 10, pp. 2289-2297, 2009.
- [18] Y.-C. Liu and Y.-M. Chen, "A systematic approach to synthesizing multi-input DC-DC converters," *IEEE Transactions on Power Electronics*, vol. 24, no. 1, pp. 116-127, 2009.
- [19] K. Gummi and M. Ferdowsi, "Double-input dc-dc power electronic converters for electric-drive vehicles—Topology exploration and synthesis using a single-pole triple-throw switch," *IEEE Transactions on Industrial Electronics*, vol. 57, no. 2, pp. 617-623, 2010.
- [20] B. Zhao, Q. Song, and W. Liu, "Power characterization of isolated bidirectional dual-active-bridge DC-DC converter with dual-phase-shift control," *IEEE Transactions on Power Electronics*, vol. 27, no. 9, pp. 4172-4176, 2012